

Convincing Rationales for Visual Question Answering Reasoning

Kun Li, George Vosselman, Michael Ying Yang
University of Twente

Abstract

Visual Question Answering (VQA) is a challenging task of predicting the answer to a question about the content of an image. It requires deep understanding of both the textual question and visual image. Prior works directly evaluate the answering models by simply calculating the accuracy of the predicted answers. However, the inner reasoning behind the prediction is disregarded in such a “black box” system, and we do not even know if one can trust the predictions. In some cases, the models still get the correct answers even when they focus on irrelevant visual regions or textual tokens, which makes the models unreliable and illogical. To generate both visual and textual rationales next to the predicted answer to the given image/question pair, we propose **Convincing Rationales for VQA, CRVQA**. Considering the extra annotations brought by the new outputs, CRVQA is trained and evaluated by samples converted from some existing VQA datasets and their visual labels. The extensive experiments demonstrate that the visual and textual rationales support the prediction of the answers, and further improve the accuracy. Furthermore, CRVQA achieves competitive performance on generic VQA datasets in the zero-shot evaluation setting. The dataset and source code will be released under <https://github.com/lik1996/CRVQA2024>.

1. Introduction

Visual Question Answering (VQA) takes as input an image and a natural language query, and predicts the corresponding answer based on the understanding of the vision-language content. Typically, answer accuracy is employed in most VQA systems [2, 17, 39] to measure the correctness of the predictions. As such, the users cannot know how reliable the answers are. In contrast, VQA with explanations tries to tie the predicted answer to the given image/question pair by providing rationales in different formats (interesting image regions [8] or textual explanations [32]). This explanatory mechanism enables VQA systems to reason for complex multi-modal scene understanding, which is comparable to human comprehension and decision process.

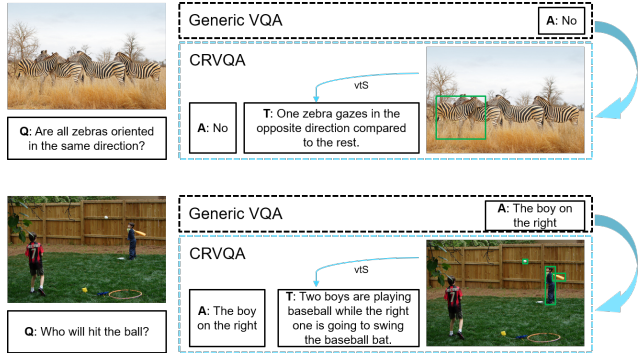


Figure 1. Illustration the difference of our CRVQA and the generic VQA. CRVQA answers the question about a related image and further predicts the textual and visual rationales to support the answering. The green bounding boxes show the involved objects for the given image/question pair. Both the visual and linguistic outputs provide explanations for VQA reasoning. *vis* represents the new metric for textual rationale evaluation.

Interpretation is considered as one of the essential properties of the recent artificial intelligent systems, and much progress has been made to achieve such an “explainable AI” purpose [47]. However, there exists a large gap for incorporating human-friendly explanations into interactive vision-language tasks such as VQA. The prevailing solutions to address this challenge are single-track methods: either from visual hints (“V-Exp”) or textual explanations (“T-Exp”). Specifically, V-Exp methods [8, 42] predict the answer to the given image/question pair, and further extract the visually interesting regions by analyzing the heat maps or attention maps in the inner neural network layers. Since the maps are representing the most salient regions when the answering system makes decisions, V-Exp methods aim to provide visual evidences by such thresholded image regions. However, the provided information is usually coarse and inaccurate and the interesting image regions (region-level) are not human-friendly for understanding the decision-making process. T-Exp methods [32, 53, 58] try to describe the visual content that helps answer the question via a short natural language sentence. Take the upper part in Fig. 1 as an example, with the predicted textual explanation “one zebra gazes ... opposite direction ... the rest”, we can easily infer the an-

swer “No” when given such an image/question pair. However, it still lacks of the rich comprehension on the vision-language input when we would like to know the specific target directly (i.e., the zebra in green bounding box). Another drawback is brought by the inconvenience of the explanation when the scene gets more complex (imagine there are more zebras lying on the ground or some horses present). Based on the above concerns in mind, we observe that the current single-track explanatory VQA methods cannot satisfy the interactive vision-language answering system. In addition, the widely-used metrics [4, 34, 41, 51] for text comparison only measure the similarity between the generated text and ground-truth by analyzing the present tokens in common for “fluency”, which cannot indicate whether they relate to the given input logically.

To generate both visual and textual rationales next to the predicted answer to the given image/question pair, in this paper we propose *Convincing Rationale for Visual Question Answering (CRVQA)*. To illustrate the difference between the generic VQA and our proposed CRVQA, two examples are shown in Fig. 1. As shown in the bottom part, both two models can predict the answer “the boy on the right” correctly. In addition, CRVQA can provide more detailed information that explains the reasoning process of the decision-making: the textual rationale “the right boy swings the baseball bat” and *the right boy, ball, and baseball bat* in green bounding boxes. We build our model on top of a Transformer architecture [50], and project the features to the latent space of a large language model for the textual prediction. We leverage a pre-trained open-vocabulary detector to accurately extract the bounding boxes for the visual rationales. Furthermore, we introduce a new metric to evaluate the generated textual rationale from both vision and language perspectives. The experimental results demonstrate the superior performance of the proposed model, and the generated textual and visual rationales are verified to improve both the model’s interpretation capability and the answer accuracy in the extensive ablation studies.

The **main contributions** of this paper are summarized as follows:

- We propose **CRVQA**, a novel VQA model that enables the system to explain the answer prediction based on both generated textual rationales (textual descriptions) and visual rationales (object-level bounding boxes).
- To measure the quality and reliability of generated textual rationales, we are the first of proposing a metric to evaluate the natural language predictions from the view of vision.
- The experiments show the effectiveness of our explainable VQA model. In addition, CRVQA generalizes well to the generic VQA task in the zero-shot evaluation setting.

2. Related Work

Visual Question Answering. Visual question answering task is commonly considered as a classification problem with the pre-defined answer candidate pool [3, 16], which relies on a simple accuracy metric to measure its performance. As the multi-modal task takes as input both images and questions, VQA models address the problem through diverse approaches in different stages, including feature extraction [2, 22], alignment [28, 36], fusion [5, 15], and prediction [23]. With the introduction and fast pace developments of self-attention Transformers [50], both natural language processing and computer vision have witnessed advances in vision-language tasks [21, 59]. Prior works [38, 52, 60] investigate leveraging the vision-language pre-training from large-scale data to enhance the efficacy of VQA models and enable complex reasoning [39], pioneering the burgeoning trend in vision-language community [40, 55]. However, these methods require access to internal parameters for fine-tuning and face the challenge in elucidating the reasoning process behind their predictions. In contrast, we explore convincing rationales to support answer predictions.

Explanations. Deep neural networks are typically “black boxes” because of the end-to-end training procedure [19]. Models with explanations enable the users to see how the inner system works. Recently, the explanatory visual question answering task [32, 42] is proposed to provide the decision process that includes either the textual explanation or the visual focus. Specifically, the textual explanation reflects the corresponding reasoning descriptions why the system predicts the answer, while the visual focus is often represented in the form of the interesting region. VQA-E [32] takes the joint representation from the input to generate the textual explanation based on an LSTM language model. Early models for visual explanations generate heat maps or attention maps that highlight the most crucial regions in an image (region-level), e.g., VQA-HAT [8] and PJ-X [42]. Recent works [6, 26, 44] leverage the large multi-modal models and pre-trained object detector or segmentor to explain the decisions visually. However, such techniques demand substantial computational resources, making them challenging to train from scratch. A recent similar work to ours is VCIN [54] that proposes a variational causal inference to build the causal correlation between the answer and explanation for VQA, which generates the restricted textual explanation but requires additional relations among the objects [7]. In contrast, our method supports the open-ended textual rationale generation only under the supervision of answers and explanations.

Localization Models with Text. Referring expression comprehension, also known as visual grounding [14], is a task of locating the targets conditioned on the provided nat-

ural language expression. Recent years have witnessed significant progress in developing models [31, 37] for such a localization problem with the textual descriptions. These models can be roughly categorized as either two-stage or one-stage methods. Two-stage methods [9, 20] first generate region proposals and then select the best matching results, while one-stage methods [12, 56] directly predict the results. However, these models rely on the specific texts to identify the target objects or categories, but the query text is not limited to the given expression. Normally, the target objects are not always mentioned in the questions for VQA. In our work, the gap is filled by the generation of the textual rationale that explains the reasoning chain with the specific involved targets.

3. Method

We propose CRVQA, an explanatory visual question answering model that generates both visual and textual rationales to support the answer prediction. We start with the problem formulation. Given an image I and a natural language question Q , our goal is to learn the predictions of (1) an answer A to this question/image pair, (2) a textual rationale TR for explaining the predicted answer in text, (3) a visual rationale VR to show the involved objects. This can be formulated as follows:

$$\{A, TR, VR\} = P(I, Q; \theta), \quad (1)$$

where θ represents the parameters of the CRVQA model.

Given the above settings, there does not exist an available dataset designed for this task. To avoid heavy human annotation effort, we build **VQA-R** (Visual Question Answering Reasoning), an explanatory VQA dataset synthesized with a matching procedure. In this section, we first introduce the process of data synthesis. Then we elaborate the proposed CRVQA network in detail. Finally, a new metric on textual rationale evaluation is introduced.

3.1. VQA-R Dataset Synthesis

We review the available explanatory VQA datasets [6, 8, 32, 42] as the source of candidates for our task. We observe that either visual evidence or textual explanation is absent or incomplete in these datasets. Then VQA-E [32] is taken as the base version because it includes sufficient numbers of answer/text pairs and the related images are from the COCO dataset [35] that supports bounding box annotations for the object detection task. We synthesize the visual rationales by matching the available annotations from COCO with the question/answer/text triplets present in the validation set (88K) of VQA-E. To ensure the quality of the matched bounding boxes, we further manually edit the results. Fig. 2 shows the overall process of VQA-R synthesis.

Specifically, we collect all the nouns present in the question/answer/text triplets from VQA-E [32]. These nouns

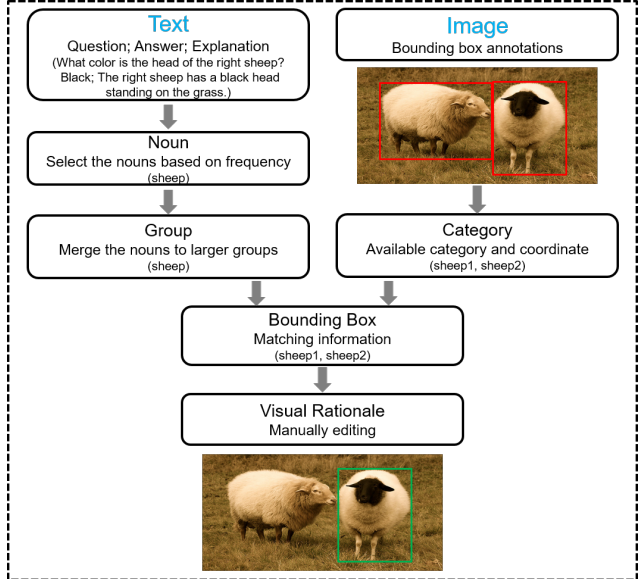


Figure 2. The overall process of VQA-R dataset synthesis. The text in the brackets and the aligned figure show an example.

always refer to the objects that are involved in the reasoning process of VQA. For instance, given a question “What color is the tie of that boy?”, the visual evidence points to the targets “tie” and “boy” shown in the image. However, analyzing all the nouns is not a practical approach as there are more than 10K categories included. We proceed to perform a frequency analysis on the nouns and select those that appear more than 20 times. With this step, we obtain 1247 different nouns that can be matched with the visual labels. Note that COCO [35] only labels 90 category objects for object detection. Then we introduce a strategy by classifying the candidate nouns into larger groups that align with the original annotations. For instance, nouns such as *man*, *woman*, *farmer*, *people*, *boy*, *girl* can be grouped to the *Person* category in COCO. Up to this step, we obtain the bounding box annotations for the image/question pairs.

However, not all the bounding boxes in one category are valid for a given image/question pair. For instance in Fig. 2, only one sheep can serve as the visual rationale given the image that includes two sheep and the question about the “right sheep”. Similarly, the extracted objects cannot always be sufficient to represent the reasoning process. For instance, given a question “What is the man doing?”, an answer “surfing” and a text “a man on the wave”, we can only extract the bounding box for the valid noun “man” as the candidate while the visual rationale should be the labels for a man and a surfboard. To ensure the quality of visual rationales, we further manually edit the bounding boxes obtained above by removing irrelevant objects and adding involved objects for explanation. Finally, we synthesize VQA-R dataset that contains 33726 image/question pairs annotated by answers, textual rationales and visual ra-

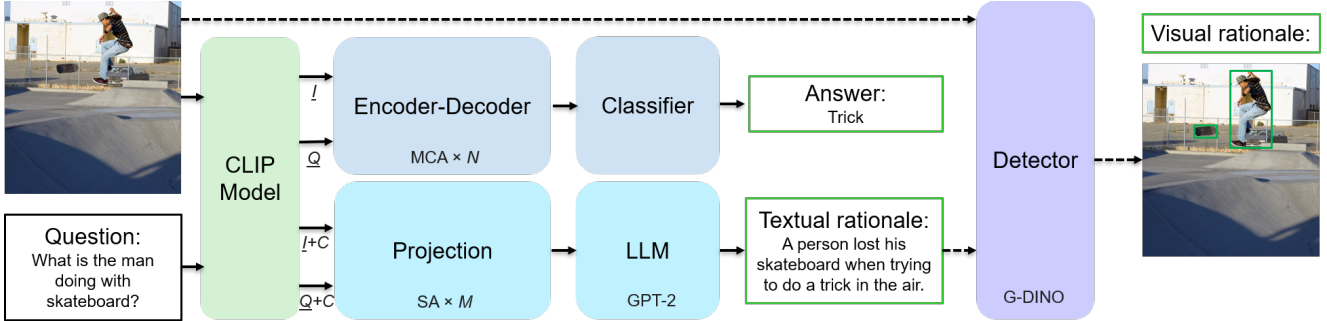


Figure 3. The framework of the proposed CRVQA model. It takes two inputs, including an image and a natural language question. \underline{I} and \underline{Q} denote the CLIP [46] representations for the image and the question, respectively. M and N represent the numbers of the attention layers. The dashed arrows indicate the flow exclusively during the inference stage. The model outputs the corresponding answer and its visual and textual rationale. Note that the parameters of CLIP model are frozen during training.

tionales for explanatory VQA. This dataset will be made publicly available. More details are provided in the supplementary material.

3.2. CRVQA Network

The overall framework of the proposed CRVQA is shown in Fig. 3. In the following section, we introduce its input representations, encoder-decoder, projection module, predictors, and loss functions.

Input Representations. The CLIP (Constractive Language-Image Pre-training) [46] model is pre-trained on large-scale image/caption pairs, demonstrating its power in vision-language tasks compared with visual encoders purely trained on in-domain data. Inspired by [48], we employ a pre-trained CLIP model to extract the visual and textual features from the input image and question, respectively.

Encoder-Decoder. For the VQA training part, we build the network on top of several Modular Co-Attention layers (MCA) proposed in [57]. The MCA layer refers to a modular composition of self-attention units and guided-attention units. The self-attention unit extracts intra-modal features for either vision or language modality, while the guided-attention unit facilitates cross-modal interactions.

Projection Module. The projection module refers to the connection part between the pre-trained models and the large language model in recent vision-language works. A simple linear projection is widely used and has been demonstrated to be effective in various scenarios [27]. We propose a Transformer-based module to project the CLIP [46] features to the latent space of a large language model (GPT-2 [45], discussed below). We leverage the self-attention mechanism in Transformers, which enables the learning of global features between tokens even in the context of long sentences. In our scenario, this capability can enhance the projection when dealing with complex questions. As the input for the projection module, we utilize the CLIP vi-

sual and question representations, \underline{I} and \underline{Q} respectively, along with two additional learned constant inputs. The constant inputs help extract the robust and valuable CLIP embeddings via the Transformers. We employ eight self-attention layers for the dual vision-language branch. The self-attended features I_{proj} and Q_{proj} are calculated as follows:

$$I_{proj} = SA(Cat(\underline{I}, C)), \quad (2)$$

$$Q_{proj} = SA(Cat(\underline{Q}, C)), \quad (3)$$

$$SA(q, K, V) = Softmax\left(\frac{qK}{\sqrt{d}}\right)V, \quad (4)$$

where C represents the learned constant input. We concatenate the projected features f_{proj} before feeding them into GPT-2.

Predictors. As the predictions consist of answers, textual rationales, and visual rationales, we use different predictors in our framework. For the answer prediction, we treat it as a classification problem like the prior methods [2, 5] and adopt a linear fusion module followed by a sigmoid function proposed in [57]. To generate the textual rationales, we utilize an auto-regressive large language model, GPT-2 [45] that predicts the next token without taking future tokens into account. For each current token in the text, GPT-2, conditioned on the projected features, produces probability scores for all vocabulary tokens, and these scores are utilized to determine the subsequent token. The prediction of visual rationales is based on an open-vocabulary object detector, Grounding-DINO [37], which can detect arbitrary objects with manual inputs. Given the input image and the generated textual rationale, we leverage such a powerful detector to localize the involved objects with bounding boxes. The distinction from referring object detection [14] is that we treat the detected bounding boxes as single category. There are two reasons behind this: (1) it is hard to analyze the category of involved objects based on the input question, for instance, a question like ‘‘What color is this object?’’; (2)

the descriptions of the objects in the textual rationale are inconsistent from various perspectives.

Loss Functions. In the training stage, we optimize the model under full supervision of answers and textual rationales with different loss functions. For VQA, the sigmoid function predicts the score \hat{s} in the range from 0 to 1 as the probability of the answer. We adopt the widely-used binary cross-entropy loss [49] for answering. To learn the explanation generation, we employ the simple yet effective cross-entropy loss based on the projection module and the GPT-2 [45] language model. Given M questions, N candidate answers, M textual rationales, the answering loss L_{ans} and explanation generation loss L_{tr} are:

$$L_{ans} = - \sum_i^M \sum_j^N s_{ij} \log(\hat{s}_{ij}) - (1 - s_{ij}) \log(1 - \hat{s}_{ij}), \quad (5)$$

$$L_{tr} = - \sum_i^M \sum_t^l \log p_{\theta}(w_t^i | f_{proj}^i, w_1^i, \dots, w_{t-1}^i), \quad (6)$$

where l, θ represent the maximum length of tokens and the trainable parameters, respectively. The sequenced tokens are referred as $w^i = w_1^i, \dots, w_l^i$. To train the entire model for multi-task learning, we take the linear combination of the answering loss L_{ans} and explanation generation loss L_{tr} as follows:

$$L = L_{ans} + L_{tr}, \quad (7)$$

3.3. Visual-Textual Similarity Score

Prior methods for text generation task commonly adopt the language evaluation metrics, such as BLEU [41] and SPICE [1]. Recently, with the advance of the embedding and transcription models in the field of natural language processing, the similarity score between the sentence embeddings can be a good option to measure the quality of the generated text. For instance, pre-trained BERT [10] is good at converting the text to dense vectors that can be used to calculate the distance between two sentences. We employ a powerful pre-trained text embedding model, GTE [33], to project the generated textual rationale to the high-dimensional space, and utilize the cosine similarity score to measure the textual similarity compared with the ground truth. Furthermore, we assess the quality of the generated texts from a visual standpoint. Specifically, the predicted bounding boxes are compared with the ground truth by calculating the Average Precision (AP) [13]. We introduce a new metric **vtS** (visual-textural Similarity score), to assess the generated textual rationales, providing a comprehensive measure of VQA reasoning capability. Given the generated textual rationale P , ground-truth GT , the metric **vtS** is defined as follows:

$$vtS = \frac{2 \times \cos(\text{GTE}(P, GT)) \times AP}{\cos(\text{GTE}(P, GT)) + AP}, \quad (8)$$

4. Experiments

4.1. Experiment Setup

Datasets. We evaluate our proposed CRVQA on three datasets, namely VQA-R, VQA-X [42], and VQAv2 [17]. VQA-R is built on top of VQA-E [32] as discussed in Sec. 3.1. Bounding box annotations are supported in the test stage to analyze the quality of the textual rationales and the visual rationales. VQA-X [42] contains 30K image/question pairs and their corresponding textual explanations, which are human-annotated and of high quality. VQAv2 [17] is a widely-used VQA benchmark dataset that includes 110K image/question pairs. It only supports the answer prediction evaluation.

Implementation Details. We adopt the visual encoder of the pre-trained CLIP [46] model with the ViT [11] base version for the image representation. We also use the CLIP model to extract the features as the question representation. The encoder-decoder network is built on the 6-layer self-attention and cross-attention Transformers inspired by MCAN [57]. We use the AdamW [25] optimizer with the learning rate of 2×10^{-5} . All the models are trained for 50 epochs with a batch size of 64 on two A40 GPUs in the same environment.

Evaluation Metrics. As the predictions include the answer, textual rationale, and bounding box, we evaluate the performance with various metrics. For visual question answering performance, we adopt the classification accuracy and only take the multiple-choice answer as the ground truth. To evaluate the generated textual rationales, we employ five mainstream metrics, namely BLEU-4 [41], METEOR [4], ROUGE [34], CIDEr [51] and SPICE [1] (B, M, R, C, S for their abbreviations, respectively), which measure the language similarity between the generated and ground truth text. In addition, we use the newly introduced metric **vtS** to better capture the similarity by leveraging the visual information. We use the GTE-large [33] as the embedding model for calculating the textual similarity. Since the prediction of the visual rationale is treated as a single-category object bounding box for the given image/question pair, we adopt the widely-used AP [13]. To align with human preference, following [32], we also include a user study across four aspects: *fluent*, *correct*, *relevant*, and *complementary*.

4.2. Results on VQA-R and VQA-X

Considering the different predictions for this task, we report the results on VQA-R and VQA-X in three parts.

Table 1 shows the experimental results of the compared explanatory VQA methods on VQA-R dataset in terms of various textual rationale evaluation metrics. Note that CRVQA-v1 and CRVQA-v2 denote the model only trained and predicted for the answer and the textual rationale, re-

Table 1. Results on VQA-R for evaluating the textual rationale generation, with the image/question representation and text predictor each method uses. B, M, R, C, S, and vtS are abbreviated for BLEU-4 [41], METEOR [4], ROUGE [34], CIDEr [51], SPICE [1], and visual-textual Similarity score. All scores are reported in percentage (%). The best results are highlighted in **bold**.

Method	V-Features	Q-Features	T-Predictor	B	M	R	C	S	vtS
PJ-X [42]	CNN	LSTM	LSTM	8.78	16.94	35.65	89.31	15.32	49.19
VQA-E [32]	CNN	GRU	LSTM	8.93	17.02	35.96	90.84	16.83	51.88
FME [53]	CNN	GRU	LSTM	12.81	21.26	37.69	89.16	18.77	53.82
CCM [43]	CNN	LSTM	LSTM	8.85	17.86	38.42	92.46	18.35	54.44
DMRFNet [58]	CNN	GRU	GRU	13.34	19.44	40.76	95.68	20.41	56.06
CRVQA-v2	CLIP	CLIP	GPT	15.08	21.77	42.04	102.86	21.22	57.30
CRVQA-v3	CLIP	CLIP	GPT	15.84	22.41	43.57	105.31	22.19	58.19

spectively, while the CRVQA-v3 represent the combined version. We observe that our proposed methods boost the performance of the text similarity (B, M, R, C, S) compared to the prior methods. With the help of the CLIP [46] model for the input representation and the GPT-2 [45] language model for the text generation, our method trained for only textual rationales (CRVQA-v2) improves the scores as well. In addition, our method achieves the highest vtS score over the comparison methods with the better quality of the generated textual and visual rationales. In turn, it helps to evaluate the reliability of the predicted answer and the generated explanation.

Table 2 compares the proposed method with other VQA models on VQA-R dataset in term of answer accuracy. The upper part reports the performance of the models trained for generic VQA. The methods in bottom part support not only the answer prediction but the textual explanation generation. Due to the fact that no specifics regarding the implementation details of answer prediction or the associated VQA accuracy are reported in PJ-X [42], FME [53] and CCM [43], we do not show the corresponding scores in Tables 2 and 3. Our proposed method (CRVQA-v3) achieves 74.81% overall accuracy and outperforms other methods on VQA-R. The boosting scores for “Yes/No” and “Other” category questions (3.60% and 0.89%, respectively) validate the effectiveness of the proposed method. We emphasize that the textual rationale generation can enhance answer accuracy, as demonstrated by comparing the results of CRVQA-v1 and CRVQA-v3. We argue that the additional supervision of textual rationales can provide more information that the answering model needs.

We further compare the results with other explanatory VQA methods on VQA-X [42] in Table 3. From this table, we can observe similar phenomenon in which our proposed method outperforms all prior methods on both the answer accuracy and the text similarity scores. Although the scale of VQA-X is much smaller than VQA-E [32], we believe that with more high-quality annotations, our method can generate more robust and reliable textual rationales to

Table 2. Results on VQA-R for answer accuracy. The methods on top are trained only for answer prediction, while the methods below are designed for answers as well as textual explanations. OA and AA represent overall and average accuracy, respectively.

Method	Number	Yes/No	Other	OA	AA
MUTAN [5]	49.23	65.52	60.27	61.07	58.34
BUTD [2]	52.68	64.07	65.72	64.13	60.83
BAN [24]	54.45	67.81	68.63	67.22	63.63
MCAN [57]	59.19	71.70	72.37	71.09	67.76
BLIP [29]	63.68	72.43	74.83	73.16	70.31
VQA-E [32]	54.26	63.98	66.45	64.67	61.57
DMRFNet [58]	59.08	72.28	73.84	72.15	68.40
CRVQA-v1	57.02	72.80	73.41	71.89	67.75
CRVQA-v3	63.20	76.03	75.72	74.81	71.65

Table 3. Results on VQA-X [42] test set for answer and textual rationale accuracy. The best results are highlighted in **bold**.

Method	B	M	R	C	S	OA
PJ-X [42]	19.5	18.2	43.7	71.3	15.1	-
VQA-E [32]	20.7	18.6	44.2	75.6	15.6	70.2
FME [53]	24.4	19.5	47.4	88.8	17.9	-
CCM [43]	21.1	19.7	44.9	73.9	16.2	-
DMRFNet [58]	20.5	19.9	41.3	74.5	17.6	72.6
CRVQA-v2	26.2	21.2	46.3	99.6	18.8	-
CRVQA-v3	26.6	22.0	48.9	98.4	19.2	78.8

support the predicted answers.

4.3. Zero-Shot Evaluation on VQAv2

We perform zero-shot evaluation on VQAv2 [17] and compare the results with prior methods in Table 4. The upper part shows the methods either directly trained or pre-trained on large-scale data and then fine-tuned on VQAv2. The results get better with more powerful models and data. For instance, pre-training with more than 129M image/text pairs, BLIP [29] can improve the accuracy to 78.3% after the downstream fine-tuning. The methods listed in the bot-

Table 4. Comparison with state-of-the-art methods on VQAv2 [17] test-dev. T-Data and T-Scale represent the training dataset and the image/question pairs. Multiple includes pre-training vision-language datasets (129M* images) as stated in [29].

Method	T-Data	T-Scale	Fine-tuned?	OA
BUTD [2]	VQAv2	443K	✗	65.3
VQA-E [32]	VQAv2	443K	✗	66.2
TRAR [61]	VQAv2	443K	✗	72.6
BLIP [29]	Multiple	129M*	✓	78.3
VQA-E [32]	VQA-E	181K	✗	62.5
DMRFNet [58]	VQA-E	181K	✗	62.9
BLIP2 [30]	Multiple	129M*	✗	65.0
CRVQA-v1	VQA-E	181K	✗	63.2
CRVQA-v3	VQA-E	181K	✗	64.7

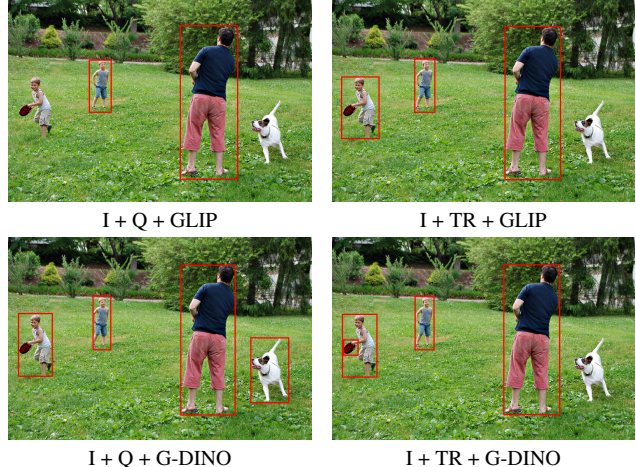
tom part are reported with the zero-shot evaluation performance. These methods are trained on other datasets then evaluated on VQAv2. We can observe that even with quite limited training data, our method can achieve competitive results (64.7%) for generic VQA in the zero-shot setting. The comparison with the large pre-training model BLIP2 [30] also validates the effectiveness of incorporating the textual rationales in the answering system. We believe that training with large-scale data can further enhance the answering performance under the new task settings.

4.4. Ablation Studies

We conduct ablation studies to quantify the performance gain resulting from different components in our proposed method. We design several variants: Question or textual Rationale for GLIP [31] and Grounding-DINO [37]; visual-textual Similarity score or User Study for the evaluation.

Question vs. Textual Rationale. To analyze the effectiveness of the generated textual rationale as the text input for open-vocabulary detectors (GLIP [31], Grounding-DINO [37]), we conduct experiments on VQA-R using either questions or textual rationales. Table 5 shows the comparison results with average scores. We can observe that both detectors are struggling with question inputs that cannot offer complete and clear object information. Our generated textual rationales largely bridge the gap for pre-trained grounding models, resulting in a 13% performance improvement. In addition, Fig. 4 shows an example for the qualitative comparison. Although there are slight performance gaps between different detectors, they can achieve better results with clearer and richer text.

vtS Score vs. User Study. To further evaluate the quality of the generated textual rationales and the confidence of our proposed metric (vtS), we conduct experiments to determine the consistency of the texts in explanations with the



Question: What are the crowds doing?

Answer: Playing frisbee.

textual Rationale: A father plays frisbee with his two sons.

Figure 4. Examples of visual rationales generated by different detectors (GLIP [31], G-DINO [37]) with question (Q) or textual rationale (TR) as the text input. We use the red bounding boxes to better visually show the involved objects because of the green background of the image (I).

Table 5. Results on VQA-R for visual rationale accuracy (AP) with respect to different inputs for open-vocabulary detectors. We feed either “question” or “textual rationale” as the language query for detectors. G-DINO is short for Grounding-DINO [37].

Image	Question	Textual Rationale	Detector	AP
✓	✓		GLIP	32.06
✓		✓	GLIP	44.17
✓	✓		G-DINO	32.57
✓		✓	G-DINO	45.86

predicted answers. We randomly select 200 samples from VQA-R, and predict the answers, textual and visual rationales. In our user study, we employ three annotators to evaluate the quality of the texts across four aspects [32] (*Fluent*, *Correct*, *Relevant*, *Complementary*), using a grading system that ranges from 1 to 5, where 1 represents “very poor” and 5 signifies “very good”. *Fluent* indicates the fluency of the text in grammar, while *Correct* represents whether the text is correct based on the image content. *Relevant* measures the relevance of the text to the image/question pair, while *Complementary* assesses whether the text makes the answering complete and easy to understand. Note that we perform the same process for the ground truth, and calculate the vtS score as well to assess the quality of VQA-R. Table 6 reports the results, and we can observe that the quality of the textual rationales is good for human preference compared to the previous method [58]. The vtS scores are also consistent with the human evaluation results. Note that for

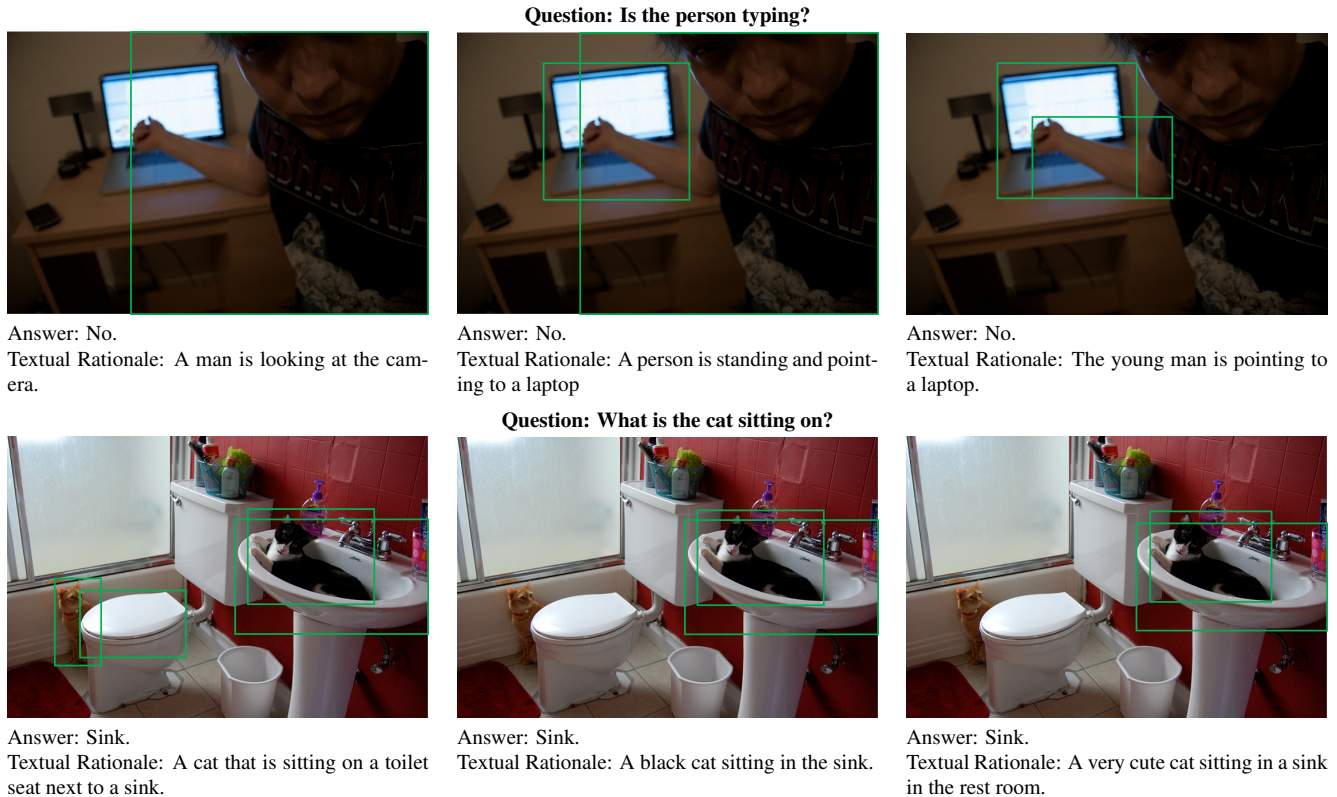


Figure 5. Qualitative results of our model (*Middle*) compared to the ground truth (*Right*) and DMRFNet [58] (*Left*) on VQA-R. The green bounding boxes show the visual rationales for the given image/question pair.

Table 6. Comparison results between user study and the proposed visual-textual Similarity (vtS) score. Here shows the average performance of the 200 samples. Corre., Relev. and Compl. are abbreviated for *Correct*, *Relevant* and *Complementary*, respectively.

Method	Fluent	Corre.	Relev.	Compl.	vtS (%)
DMRFNet [58]	3.29	3.33	3.16	3.09	55.63
CRVQA-v3	3.56	3.42	3.34	3.25	58.87
GT	4.64	4.44	4.04	3.93	80.82

the last row we feed the detector with ground truth textual rationales to generate the bounding-boxes, then we calculate AP by the synthesized ground-truth labels while setting the value of $\cos(\text{GTE})$ to 1.

4.5. Qualitative Analysis

We conduct a qualitative analysis on the predicted answers and rationales. Fig. 5 illustrates two specific examples from VQA-R, comparing our proposed model with DMRFNet [58]. For both image/question pairs, DMRFNet is able to predict the correct answers, but fails to generate the corresponding textual rationale and visual evidence. In the bottom part, DMRFNet generates a wrong textual explanation (“sitting on a toilet seat”) but still predicts the correct answer. Our model can comprehend the given im-

age/question pairs exactly and generate reasonable explanations for the answers. For example, when our model correctly understands the image’s content and the query, it can discern the relationship between “the laptop” and “the person”. Although the visual evidence is not perfectly accurate (“hand” or “entire body”), the generated text indicates the process of the answering.

5. Conclusion

In this paper we propose a VQA reasoning method (**CRVQA**) that predicts not only the answer but the textual and visual rationales to support the answering. To reduce the efforts for annotating the visual labels, we synthesize a dataset for VQA reasoning with a matching procedure. We leverage a large language model to generate the textual rationale and an open-vocabulary detector to extract the visual evidence. We demonstrate the effectiveness of the proposed CRVQA on VQA reasoning. Furthermore, we introduce a new metric to measure the quality of the generated textual explanations from the view of vision. The experiments conducted on three VQA datasets demonstrate that our method achieves the superior performances compared to the previous approaches. In addition, CRVQA generalizes well to the generic VQA task in the zero-shot evaluation setting.

Appendix

In this supplementary document, we provide detailed explanations on the synthesized VQA-R dataset in Sec. A. Additional ablation studies in terms of the projection module, the introduced metric vtS, and frozen/fine-tuning language model are provided in Sec. B. Moreover, we also provide more qualitative results in Sec. C.

A. Synthesized VQA-R Dataset

In this section, we analyze our synthesized VQA-R dataset, compared with the prior explanatory VQA datasets. We collect the question/answer/explanation triplets from the validation of VQA-E [32] and match them with the available visual labels followed a manual editing step as discussed in the main text. There are 33726 image/question pairs well annotated in total in VQA-R. More detailed statistics about the dataset are given in Table 7. We can see that the proposed VQA-R dataset supports the answering as well as the visual and textual explanations in accurate and sufficient bounding box annotations.

B. Additional Ablation Study

We further report three groups of ablation studies with respect to the projection, metric, and language model.

Projection Module. In the main text, we adopt a transformer projection module to project the features to the latent space of GPT-2 [45] model. To measure the effectiveness of the proposed Transformer blocks, we conduct an ablation study by comparing the results with that of a linear projection that the prior methods [27, 44] adopt. The results are reported in Table 8. We observe that the proposed Transformer-based projection module can enhance the performance compared to the widely-used linear module on different metrics (e.g., 2.34% on the introduced vtS).

Metrics. To measure the generated textual rationale, we first introduce a metric called vtS (discussed in the main paper). Here we further consider the different combination of visual (AP) and textual (GTE similarity) aspects. Specifically, there are three options: (1) simply summarizing AP and $\cos(GTE)$ then divided by two; (2) multiplying AP and $\cos(GTE)$; (3) dividing the result from (2) with that from (1), and we name it vtS in this paper. We report the results in Table 9, and we observe that either (1) or (2) cannot sufficiently reflect the real performance of both visual and textual branches if the two items differ too much. Therefore, we adopt a the combination format in (3) as we introduced in the main paper.

Language Model. We train the proposed model with learnable parameters of the projection module to project the pre-trained CLIP [46] features to the space of GPT-2 [45]. To

further figure out the role of the large language model GPT-2, we design an ablation study with or without fine-tuning its parameters during the training stage. The results are reported in Table 10 in terms of various evaluation metrics. Although it takes more effort to train the language predictor on VQA-E [32], the quality of the generated textual rationales is improved. For instance, the performance gain on VQA-R for CIDEr [51] score is 16.06%. Similarly, fine-tuning the language model supports better textual information for extracting the visual evidence, as shown by the vtS score improvement (5.12%).

C. More Qualitative Results

We also provide more qualitative results of the proposed CRVQA on VQA-R. Fig. 6 shows some common cases. These examples verify that CRVQA not only supports the answering but also provides robust and reliable visual and textual rationales to explain the prediction process. For instance, even there is no category-level information present in the first question, the proposed method still predicts the correct answer next to a textual explanation and visual bounding-boxes (especially for “tennis racket”). We also show a failure case (the last example in Fig. 6). Our method predicts a wrong answer “car”, but it provides the corresponding explanations for the users to make a further judgement whether the answer is correct. This case also highlights the significance of the reliability of a VQA model in contrast to a “black box” answering system.

Table 7. Statistics for the proposed VQA-R dataset. VizWiz-VQA [18] and VQA-Therapy [6] collect the images from the same mobile phone platforms. We use “-” to represent the missing data from different datasets. VR and B-box are abbreviated for visual rationale and bounding-box.

Dataset	Image Source	#Image	#Question/Answer	#Textual Rationale	#Visual Rationale	VR Format
VQA-HAT [8]	COCO	20,508	59,457	-	62,597	Region
VQAv2 [17]	COCO	204,721	1,105,904	-	-	-
VQA-E [32]	COCO	108,325	269,786	269786	-	-
VQA-X [42]	COCO	28,180	32,886	41,817	6,000	Region
VizWiz-VQA [18]	Phone	9,998	9,998	-	9,998	Boundary
VQA-Therapy [6]	Phone	5,787	5,825	-	9,537	Boundary
VQA-R	COCO	20,367	33,726	33,726	93,377	B-box

Table 8. Results on VQA-R for ablation study on the linear and Transformer projection module. B, M, R, C, S, and vtS are abbreviated for BLEU-4 [41], METEOR [4], ROUGE [34], CIDEr [51], SPICE [1], and visual-textual Similarity score. All scores are reported in percentage (%).

Method	B	M	R	C	S	vtS
Linear	14.60	21.04	42.72	98.84	20.29	55.85
Transformer	15.84	22.41	43.57	105.31	22.19	58.19

Table 9. Results on VQA-R for ablation study on the different combination of the visual and textual aspects. (1), (2), and (3) are detailed in Sec. B.

Method	AP	cos(GTE)	(1)	(2)	(3)
PJ-X [42]	38.43	68.32	53.38	26.26	49.19
VQA-E [32]	40.65	71.67	56.16	29.13	51.88
FME [53]	42.57	73.16	57.87	31.14	53.82
CCM [43]	43.08	73.94	58.46	31.85	54.44
DMRFNet [58]	44.74	75.06	59.90	33.58	56.06
CRVQA-v3	45.86	79.57	62.72	36.49	58.19

Table 10. Results on VQA-R for ablation study on the frozen and fine-tuning language models.

Method	B	M	R	C	S	vtS
Frozen	13.31	19.63	36.91	89.25	19.08	53.07
Fine-tuning	15.84	22.41	43.57	105.31	22.19	58.19

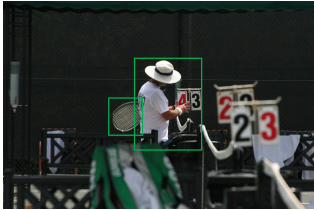
References

- [1] Peter Anderson, Basura Fernando, Mark Johnson, and Stephen Gould. Spice: Semantic propositional image caption evaluation. In *Proceedings of the European Conference on Computer Vision*, pages 382–398, 2016. 5, 6, 10
- [2] Peter Anderson, Xiaodong He, Chris Buehler, Damien Teney, Mark Johnson, Stephen Gould, and Lei Zhang. Bottom-up and top-down attention for image captioning and visual question answering. In *Proceedings of the IEEE conference on computer vision and pattern recognition*, pages 6077–6086, 2018. 1, 2, 4, 6, 7
- [3] Stanislaw Antol, Aishwarya Agrawal, Jiasen Lu, Margaret Mitchell, Dhruv Batra, C Lawrence Zitnick, and Devi Parikh. Vqa: Visual question answering. In *Proceedings of the IEEE international conference on computer vision*, pages 2425–2433, 2015. 2
- [4] Satanjeev Banerjee and Alon Lavie. Meteor: An automatic metric for mt evaluation with improved correlation with human judgments. In *Proceedings of the acl workshop on intrinsic and extrinsic evaluation measures for machine translation and/or summarization*, pages 65–72, 2005. 2, 5, 6, 10
- [5] Hedi Ben-Younes, Rémi Cadene, Matthieu Cord, and Nicolas Thome. Mutan: Multimodal tucker fusion for visual question answering. In *Proceedings of the IEEE international conference on computer vision*, pages 2612–2620, 2017. 2, 4, 6
- [6] Chongyan Chen, Samreen Anjum, and Danna Gurari. Vqa therapy: Exploring answer differences by visually grounding answers. In *Proceedings of the IEEE/CVF International Conference on Computer Vision*, pages 15315–15325, 2023. 2, 3, 10
- [7] Shi Chen and Qi Zhao. Rex: Reasoning-aware and grounded explanation. In *Proceedings of the IEEE/CVF Conference on Computer Vision and Pattern Recognition*, pages 15586–15595, 2022. 2
- [8] Abhishek Das, Harsh Agrawal, Larry Zitnick, Devi Parikh, and Dhruv Batra. Human attention in visual question answering: Do humans and deep networks look at the same regions? *Computer Vision and Image Understanding*, 163: 90–100, 2017. 1, 2, 3, 10
- [9] Chaorui Deng, Qi Wu, Qingyao Wu, Fuyuan Hu, Fan Lyu, and Mingkui Tan. Visual grounding via accumulated attention. In *Proceedings of the IEEE conference on computer vision and pattern recognition*, pages 7746–7755, 2018. 3
- [10] Jacob Devlin, Ming-Wei Chang, Kenton Lee, and Kristina Toutanova. Bert: Pre-training of deep bidirectional transformers for language understanding. *arXiv preprint arXiv:1810.04805*, 2018. 5
- [11] Alexey Dosovitskiy, Lucas Beyer, Alexander Kolesnikov, Dirk Weissenborn, Xiaohua Zhai, Thomas Unterthiner,

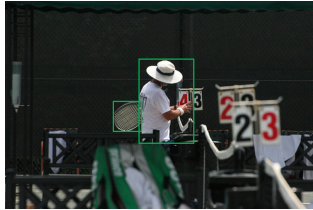
- Mostafa Dehghani, Matthias Minderer, Georg Heigold, Sylvain Gelly, et al. An image is worth 16x16 words: Transformers for image recognition at scale. *arXiv preprint arXiv:2010.11929*, 2020. 5
- [12] Ye Du, Zehua Fu, Qingjie Liu, and Yunhong Wang. Visual grounding with transformers. In *2022 IEEE International Conference on Multimedia and Expo (ICME)*, pages 1–6. IEEE, 2022. 3
- [13] Mark Everingham, Luc Van Gool, Christopher KI Williams, John Winn, and Andrew Zisserman. The pascal visual object classes (voc) challenge. *International journal of computer vision*, 88:303–338, 2010. 5
- [14] Akira Fukui, Dong Huk Park, Daylen Yang, Anna Rohrbach, Trevor Darrell, and Marcus Rohrbach. Multimodal compact bilinear pooling for visual question answering and visual grounding. *arXiv preprint arXiv:1606.01847*, 2016. 2, 4
- [15] Peng Gao, Zhengkai Jiang, Haoxuan You, Pan Lu, Steven CH Hoi, Xiaogang Wang, and Hongsheng Li. Dynamic fusion with intra-and inter-modality attention flow for visual question answering. In *Proceedings of the IEEE/CVF conference on computer vision and pattern recognition*, pages 6639–6648, 2019. 2
- [16] Yash Goyal, Tejas Khot, Douglas Summers-Stay, Dhruv Batra, and Devi Parikh. Making the v in vqa matter: Elevating the role of image understanding in visual question answering. In *Proceedings of the IEEE conference on computer vision and pattern recognition*, pages 6904–6913, 2017. 2
- [17] Yash Goyal, Tejas Khot, Douglas Summers-Stay, Dhruv Batra, and Devi Parikh. Making the v in vqa matter: Elevating the role of image understanding in visual question answering. In *Proceedings of the IEEE conference on computer vision and pattern recognition*, pages 6904–6913, 2017. 1, 5, 6, 7, 10
- [18] Danna Gurari, Qing Li, Abigale J Stangl, Anhong Guo, Chi Lin, Kristen Grauman, Jiebo Luo, and Jeffrey P Bigham. Vizwiz grand challenge: Answering visual questions from blind people. In *Proceedings of the IEEE conference on computer vision and pattern recognition*, pages 3608–3617, 2018. 10
- [19] Lisa Anne Hendricks, Zeynep Akata, Marcus Rohrbach, Jeff Donahue, Bernt Schiele, and Trevor Darrell. Generating visual explanations. In *Proceedings of the European Conference on Computer Vision*, pages 3–19, 2016. 2
- [20] Richang Hong, Daqing Liu, Xiaoyu Mo, Xiangnan He, and Hanwang Zhang. Learning to compose and reason with language tree structures for visual grounding. *IEEE transactions on pattern analysis and machine intelligence*, 44(2): 684–696, 2019. 3
- [21] Ronghang Hu and Amanpreet Singh. Unit: Multimodal multitask learning with a unified transformer. In *Proceedings of the IEEE/CVF International Conference on Computer Vision*, pages 1439–1449, 2021. 2
- [22] Huaizu Jiang, Ishan Misra, Marcus Rohrbach, Erik Learned-Miller, and Xinlei Chen. In defense of grid features for visual question answering. In *Proceedings of the IEEE/CVF conference on computer vision and pattern recognition*, pages 10267–10276, 2020. 2
- [23] Kushal Kafle and Christopher Kanan. Answer-type prediction for visual question answering. In *Proceedings of the IEEE conference on computer vision and pattern recognition*, pages 4976–4984, 2016. 2
- [24] Jin-Hwa Kim, Jaehyun Jun, and Byoung-Tak Zhang. Bilinear attention networks. *Advances in neural information processing systems*, 31, 2018. 6
- [25] Diederik P Kingma and Jimmy Ba. Adam: A method for stochastic optimization. *arXiv preprint arXiv:1412.6980*, 2014. 5
- [26] Xin Lai, Zhuotao Tian, Yukang Chen, Yanwei Li, Yuhui Yuan, Shu Liu, and Jiaya Jia. Lisa: Reasoning segmentation via large language model. *arXiv preprint arXiv:2308.00692*, 2023. 2
- [27] Chunyuan Li. Large multimodal models: Notes on cvpr 2023 tutorial. *arXiv preprint arXiv:2306.14895*, 2023. 4, 9
- [28] Dongxu Li, Junnan Li, Hongdong Li, Juan Carlos Niebles, and Steven CH Hoi. Align and prompt: Video-and-language pre-training with entity prompts. In *Proceedings of the IEEE/CVF Conference on Computer Vision and Pattern Recognition*, pages 4953–4963, 2022. 2
- [29] Junnan Li, Dongxu Li, Caiming Xiong, and Steven Hoi. Blip: Bootstrapping language-image pre-training for unified vision-language understanding and generation. In *International Conference on Machine Learning*, pages 12888–12900, 2022. 6, 7
- [30] Junnan Li, Dongxu Li, Silvio Savarese, and Steven Hoi. Blip-2: Bootstrapping language-image pre-training with frozen image encoders and large language models. *arXiv preprint arXiv:2301.12597*, 2023. 7
- [31] Liumian Harold Li, Pengchuan Zhang, Haotian Zhang, Jianwei Yang, Chunyuan Li, Yiwu Zhong, Lijuan Wang, Lu Yuan, Lei Zhang, Jenq-Neng Hwang, et al. Grounded language-image pre-training. In *Proceedings of the IEEE/CVF Conference on Computer Vision and Pattern Recognition*, pages 10965–10975, 2022. 3, 7
- [32] Qing Li, Qingyi Tao, Shafiq Joty, Jianfei Cai, and Jiebo Luo. Vqa-e: Explaining, elaborating, and enhancing your answers for visual questions. In *Proceedings of the European Conference on Computer Vision (ECCV)*, pages 552–567, 2018. 1, 2, 3, 5, 6, 7, 9, 10
- [33] Zehan Li, Xin Zhang, Yanzhao Zhang, Dingkun Long, Pengjun Xie, and Meishan Zhang. Towards general text embeddings with multi-stage contrastive learning. *arXiv preprint arXiv:2308.03281*, 2023. 5
- [34] Chin-Yew Lin. Rouge: A package for automatic evaluation of summaries. In *Text summarization branches out*, pages 74–81, 2004. 2, 5, 6, 10
- [35] Tsung-Yi Lin, Michael Maire, Serge Belongie, James Hays, Pietro Perona, Deva Ramanan, Piotr Dollár, and C Lawrence Zitnick. Microsoft coco: Common objects in context. In *Computer Vision—ECCV 2014: 13th European Conference, Zurich, Switzerland, September 6–12, 2014, Proceedings, Part V 13*, pages 740–755. Springer, 2014. 3
- [36] Fenglin Liu, Yuanxin Liu, Xuancheng Ren, Xiaodong He, and Xu Sun. Aligning visual regions and textual concepts for semantic-grounded image representations. *Advances in Neural Information Processing Systems*, 32, 2019. 2

- [37] Shilong Liu, Zhaoyang Zeng, Tianhe Ren, Feng Li, Hao Zhang, Jie Yang, Chunyuan Li, Jianwei Yang, Hang Su, Jun Zhu, et al. Grounding dino: Marrying dino with grounded pre-training for open-set object detection. *arXiv preprint arXiv:2303.05499*, 2023. [3](#), [4](#), [7](#)
- [38] Jiasen Lu, Dhruv Batra, Devi Parikh, and Stefan Lee. Vilbert: Pretraining task-agnostic visiolinguistic representations for vision-and-language tasks. *Advances in neural information processing systems*, 32, 2019. [2](#)
- [39] Kenneth Marino, Xinlei Chen, Devi Parikh, Abhinav Gupta, and Marcus Rohrbach. Krisp: Integrating implicit and symbolic knowledge for open-domain knowledge-based vqa. In *Proceedings of the IEEE/CVF Conference on Computer Vision and Pattern Recognition*, pages 14111–14121, 2021. [1](#), [2](#)
- [40] Ron Mokady, Amir Hertz, and Amit H Bermano. Clip-cap: Clip prefix for image captioning. *arXiv preprint arXiv:2111.09734*, 2021. [2](#)
- [41] Kishore Papineni, Salim Roukos, Todd Ward, and Wei-Jing Zhu. Bleu: a method for automatic evaluation of machine translation. In *Proceedings of the 40th annual meeting of the Association for Computational Linguistics*, pages 311–318, 2002. [2](#), [5](#), [6](#), [10](#)
- [42] Dong Huk Park, Lisa Anne Hendricks, Zeynep Akata, Anna Rohrbach, Bernt Schiele, Trevor Darrell, and Marcus Rohrbach. Multimodal explanations: Justifying decisions and pointing to the evidence. In *Proceedings of the IEEE conference on computer vision and pattern recognition*, pages 8779–8788, 2018. [1](#), [2](#), [3](#), [5](#), [6](#), [10](#)
- [43] Badri Patro, Shivansh Patel, and Vinay Nambodiri. Robust explanations for visual question answering. In *Proceedings of the IEEE/CVF Winter Conference on Applications of Computer Vision*, pages 1577–1586, 2020. [6](#), [10](#)
- [44] Renjie Pi, Jiahui Gao, Shizhe Diao, Rui Pan, Hanze Dong, Jipeng Zhang, Lewei Yao, Jianhua Han, Hang Xu, and Lingpeng Kong Zhang. Detgpt: Detect what you need via reasoning. *arXiv preprint arXiv:2305.14167*, 2023. [2](#), [9](#)
- [45] Alec Radford, Jeffrey Wu, Rewon Child, David Luan, Dario Amodei, Ilya Sutskever, et al. Language models are unsupervised multitask learners. *OpenAI blog*, 1(8):9, 2019. [4](#), [5](#), [6](#), [9](#)
- [46] Alec Radford, Jong Wook Kim, Chris Hallacy, Aditya Ramesh, Gabriel Goh, Sandhini Agarwal, Girish Sastry, Amanda Askell, Pamela Mishkin, Jack Clark, et al. Learning transferable visual models from natural language supervision. In *International conference on machine learning*, pages 8748–8763. PMLR, 2021. [4](#), [5](#), [6](#), [9](#)
- [47] Wojciech Samek and Klaus-Robert Müller. Towards explainable artificial intelligence. *Explainable AI: interpreting, explaining and visualizing deep learning*, pages 5–22, 2019. [1](#)
- [48] Sheng Shen, Liunian Harold Li, Hao Tan, Mohit Bansal, Anna Rohrbach, Kai-Wei Chang, Zhewei Yao, and Kurt Keutzer. How much can clip benefit vision-and-language tasks? *arXiv preprint arXiv:2107.06383*, 2021. [4](#)
- [49] Damien Teney, Peter Anderson, Xiaodong He, and Anton Van Den Hengel. Tips and tricks for visual question answering: Learnings from the 2017 challenge. In *Proceedings of the IEEE conference on computer vision and pattern recognition*, pages 4223–4232, 2018. [5](#)
- [50] Ashish Vaswani, Noam Shazeer, Niki Parmar, Jakob Uszkoreit, Llion Jones, Aidan N Gomez, Łukasz Kaiser, and Illia Polosukhin. Attention is all you need. In *Advances in Neural Information Processing Systems*, 2017. [2](#)
- [51] Ramakrishna Vedantam, C Lawrence Zitnick, and Devi Parikh. Cider: Consensus-based image description evaluation. In *Proceedings of the IEEE conference on computer vision and pattern recognition*, pages 4566–4575, 2015. [2](#), [5](#), [6](#), [9](#), [10](#)
- [52] Zirui Wang, Jiahui Yu, Adams Wei Yu, Zihang Dai, Yulia Tsvetkov, and Yuan Cao. Simvlm: Simple visual language model pretraining with weak supervision. *arXiv preprint arXiv:2108.10904*, 2021. [2](#)
- [53] Jialin Wu and Raymond Mooney. Faithful multimodal explanation for visual question answering. In *Proceedings of the 2019 ACL Workshop BlackboxNLP: Analyzing and Interpreting Neural Networks for NLP*, pages 103–112, 2019. [1](#), [6](#), [10](#)
- [54] Dizhan Xue, Shengsheng Qian, and Changsheng Xu. Variational causal inference network for explanatory visual question answering. In *Proceedings of the IEEE/CVF International Conference on Computer Vision*, pages 2515–2525, 2023. [2](#)
- [55] Jinyu Yang, Jiali Duan, Son Tran, Yi Xu, Sampath Chanda, Liquan Chen, Belinda Zeng, Trishul Chilimbi, and Junzhou Huang. Vision-language pre-training with triple contrastive learning. In *Proceedings of the IEEE/CVF Conference on Computer Vision and Pattern Recognition*, pages 15671–15680, 2022. [2](#)
- [56] Zhengyuan Yang, Boqing Gong, Liwei Wang, Wenbing Huang, Dong Yu, and Jiebo Luo. A fast and accurate one-stage approach to visual grounding. In *Proceedings of the IEEE/CVF International Conference on Computer Vision*, pages 4683–4693, 2019. [3](#)
- [57] Zhou Yu, Jun Yu, Yuhao Cui, Dacheng Tao, and Qi Tian. Deep modular co-attention networks for visual question answering. In *Proceedings of the IEEE/CVF conference on computer vision and pattern recognition*, pages 6281–6290, 2019. [4](#), [5](#), [6](#)
- [58] Weifeng Zhang, Jing Yu, Wenhong Zhao, and Chuan Ran. Dmrfnet: deep multimodal reasoning and fusion for visual question answering and explanation generation. *Information Fusion*, 72:70–79, 2021. [1](#), [6](#), [7](#), [8](#), [10](#)
- [59] Luowei Zhou, Yingbo Zhou, Jason J Corso, Richard Socher, and Caiming Xiong. End-to-end dense video captioning with masked transformer. In *Proceedings of the IEEE conference on computer vision and pattern recognition*, pages 8739–8748, 2018. [2](#)
- [60] Luowei Zhou, Hamid Palangi, Lei Zhang, Houdong Hu, Jason Corso, and Jianfeng Gao. Unified vision-language pre-training for image captioning and vqa. In *Proceedings of the AAAI conference on artificial intelligence*, pages 13041–13049, 2020. [2](#)
- [61] Yiyi Zhou, Tianhe Ren, Chaoyang Zhu, Xiaoshuai Sun, Jianzhuang Liu, Xinghao Ding, Mingliang Xu, and Rongrong Ji. Trar: Routing the attention spans in transformer for

visual question answering. In *Proceedings of the IEEE/CVF International Conference on Computer Vision*, pages 2074–2084, 2021. 7



Question: What is under his arm?
 Answer: Tennis racket.
 Textual Rationale: A man who is standing with a tennis racket.



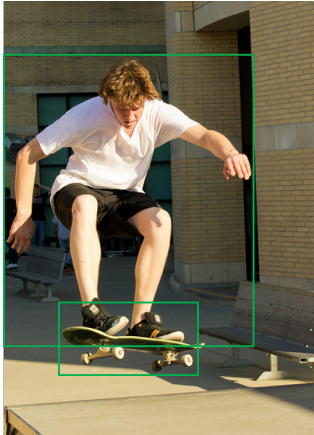
Answer: Tennis racket.
 Textual Rationale: There is a man wearing a hat holding a tennis racket.



Question: How many people?
 Answer: 2.
 Textual Rationale: Two people sitting there.



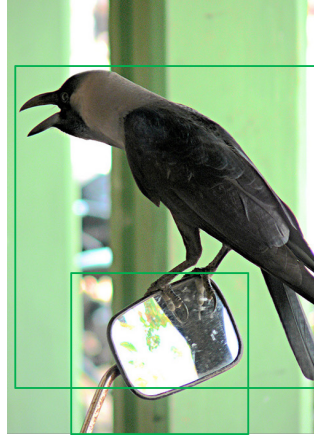
Answer: 2.
 Textual Rationale: Two people sitting on a wooden bench looking at the camera.



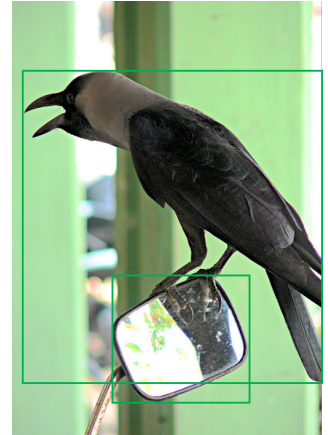
Question: What is the man doing?
 Answer: Skateboarding.
 Textual Rationale: A man is riding a skateboard on a boardwalk in a skate park.



Answer: Skateboarding.
 Textual Rationale: A skateboarder is doing stunts on a skateboard outdoors.



Question: What is the bird standing on?
 Answer: Car.
 Textual Rationale: A bird is standing on a car door.



Answer: Mirror.
 Textual Rationale: A bird standing on the side mirror of a vehicle.

Figure 6. Additional qualitative results of our CRVQA model (*Left*) compared to the ground truth (*Right*) on VQA-R. The green bounding boxes show the visual rationales for the given image/question pair. The last one shows a failure case that predicts a wrong answer.